Lab 3

Mechanical & Thermal Processing

Thursday Group 4

Partners: Bijan, Mike, Evan

Abstract:

The precipitation hardening resulted in 15T Rockwell hardness values that changed as the material aged. The initial value started at 70 HRB, then up to 82, then back down to 70. The peak value had less than a 1% error from the literature value. The cold working of our 1018 Steel was done in 4 steps achieving 17%, 36%, 67% and 79% cold worked at each. The average hardnesses at each of these steps were 130, 196, n/a, 252 and 264 HV respectively. The cold working was done in 5 steps achieving 21%, 38%, 71%, 85% and 97% cold worked at each. The average hardness at each of these steps were 35, 50, n/a, n/a, 67 and 80.2 respectively. The tensile testing was performed on two samples heated at different temperatures. The sample heated at 700°C was found to have a UTS of 454 MPa, a YS of 362 MPa, a Young's modulus of 206.85 GPa, an elongation of 26%, and a hardening exponent of 0.1731. The sample heated at 925°C was found to have a UTS of 388.5 MPa, a YS of 260.7 MPa, a Young's modulus of 204.3 GPa, an elongation of 26%, and a hardening exponent of 0.2525. The error for UTS and YS of the 700°C was roughly 3% compared to cold worked 1018 steel and the error for UTS and YS of the 925°C sample was only around 1.5% compared to annealed 1020 steel.

Objectives and Goals

The objective of this lab was to observe how one can change the properties of a material both thermally and mechanically using a variety of processes: cold rolling, annealing, and precipitation hardening. Intensive data collection was performed throughout these experiments, such that the quantitative and qualitative changes in the properties of the materials could be analyzed in depth. The goals for this lab were to demonstrate our understanding of the different processing techniques. An understanding of how this affects microstructure, crystal structure, and associated mechanical properties, was also demonstrated.

Specifically, the goals and objectives for annealing was to understand the role of temperature in the annealing process along with the different phases of annealing. For cold rolling the goal was to understand how plastic deformation affected microstructure and mechanical properties. For precipitation hardening the goal was to understand the role of beta particles in a material and how they are affected by temperature.

Introduction

The mechanical properties of materials depend on a wide assortment of variables. The mechanical properties which were investigated in this lab include hardness and tensile strength. These properties are correlated with one another such that processing which changes the value of one property will also affect the value of the other. Processing can be done in four ways: altering chemical composition, using strain, using temperature, and mixing materials. The specific processes in question were of the strain and temperature categories. The possible processing that can be done to a material depends on its intrinsic properties, as are the effects of such processing. One must however be considerate of processing as (for pure metal samples) it will alter the electrical and thermal conductivities negatively. This is not the case when developing extrinsic behaviour in an intrinsic semiconductor.

The materials used in this lab were 1018 Steel and 6061 Aluminum. The composition of both of these materials is referenced in group 2D's lab 1A. 1018 Steel is used in many industrial applications where high strength is needed due to its extreme toughness and strength; machinery and objects designed to take high impacts are often made of this alloy. Aluminum 6061 on the other hand is very light while still being quite strong. . This allows aluminum to be useful in applications where strength is required but weight is important such as in the aerospace or wind power industries.

One of the variables that affects the strength and hardness of a material is grain size. Metals, full of dislocations, have local domains of aligned dislocations. Each domain is called a grain and the interface between grains is called a grain boundary. Grain boundaries are composed of a series of angular mismatches between dislocations originating from the contacting grains **(Fig 1)**.

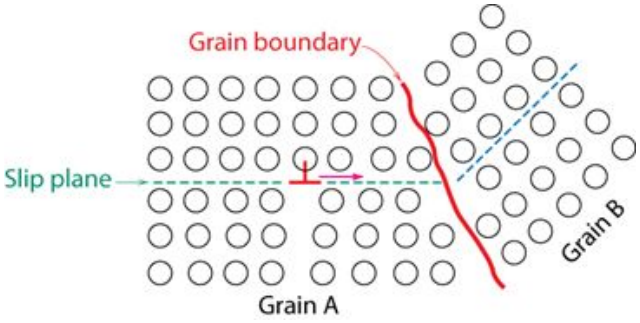

Fig. 1: grain boundary diagram

This is significant in the field of Materials Science due to the fact that grain boundaries block dislocation motion and blocking dislocation motion is one of the main ways to strengthen a material. The Orowan equation describes the behaviour of dislocation motion and is thus helpful for determining rheology of such materials. One can intuitively see how crucial dislocation motion is for plastic flow and how blocking dislocations makes materials stronger since uninterrupted they could propagate through a material until it fractures. Therefore affecting grain size will affect the density of grain boundaries in a material, changing the material's resistance to dislocation motion. Grain size strengthening can be quantified by the Hall-Petch equation **(Eq. 1)**

$$\sigma_y = \sigma_0 + \frac{k_y}{d^2} \quad \textbf{[1]}$$

Where σ_y = yield stress, σ_0 = lattice resistance to dislocation motion, k_y= strengthening coefficient d = avg. grain diameter.

This confirms our observation in this lab that decreasing grain size increases strength of a material. Mechanisms for altering grain size include stressing the material (cold rolling) and changing the temperature of the material (annealing).

Cold rolling deforms the material under stress and thereby introduces dislocations, changes in grain structure, and voids in the material. The tradeoff for hardness is a reduction in its ductility. The process for cold rolling can be seen in **(Fig. 2)** , where the material is pushed through rolling pins that stretch and plastically deform the material.

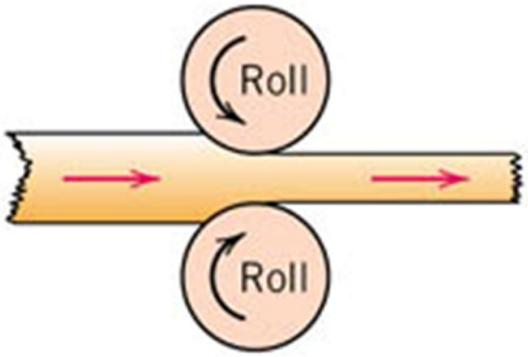

Fig. 2: cold rolling diagram

Doing this to a material without heating it is called cold working (CW). Working a material this way not only changes the microstructure from plastic deformation, but also adds many dislocations. From Callister;it is seen that a carefully solidified metal crystal has 1,000 dislocations per mm^2 while a heavily worked metal has 1,000,000,000 dislocations per mm^2. The specific changes in microstructure will be more thoroughly covered later in the report.

Annealing occurs in 3 stages. The first, recovery, softens the material through eliminating linear dislocations and the internal stresses they generate. The second stage is recrystallization, wherein strain-free grains grow to replace deformations in the changed grains after recovery. If annealing is allowed to continue uninterrupted, grains will grow larger and larger. The specific mechanisms for annealing 1018 steel and Aluminum 6061 were mentioned in lab 2D's 1a and 1b reports.

Another property that affects dislocation motion, and thus the strength and hardness of a material involves secondary (beta) particles in a material. In this case the dislocations are pinned not only by grain boundaries but also by precipitated particles. This composition is known as a solid solution due to the distribution of these beta particles. Solid solution strengthening involves alloying a material with a new element in order to introduce these beta particles. This lab specifically did not require us to alloy anything due to the fact that we were given Aluminum 6061 which is already an alloy. Therefore the processing performed was precipitation hardening. Precipitation hardening is done in 2 steps, first an initial solution heat treatment and then an accelerated aging process as seen in **(Fig. 3)**.

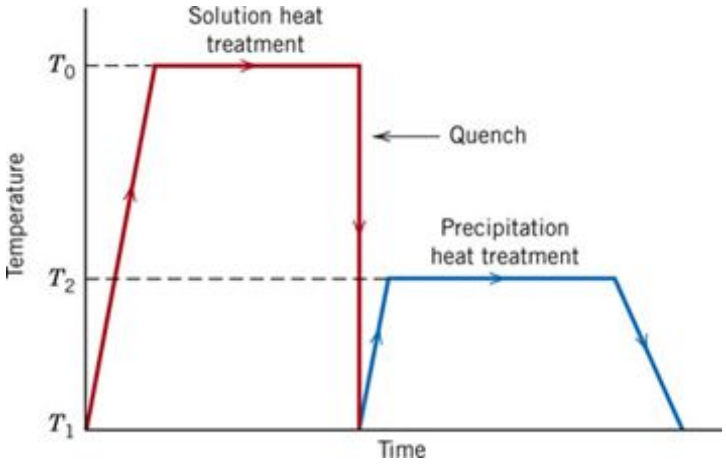

Fig. 3: heat cycling plot

The quenching is necessary to prevent diffusion since the first step brings the material to a high enough temperature to form a homogeneous solution of all the particles. Aging a material will redistribute the beta particles but it takes a long time. Keeping the material at high temperatures for extended amounts of time thermodynamically accelerate this process. **(Fig. 4)** shows this process in a phase diagram to clarify the segregation of alpha and beta particles.

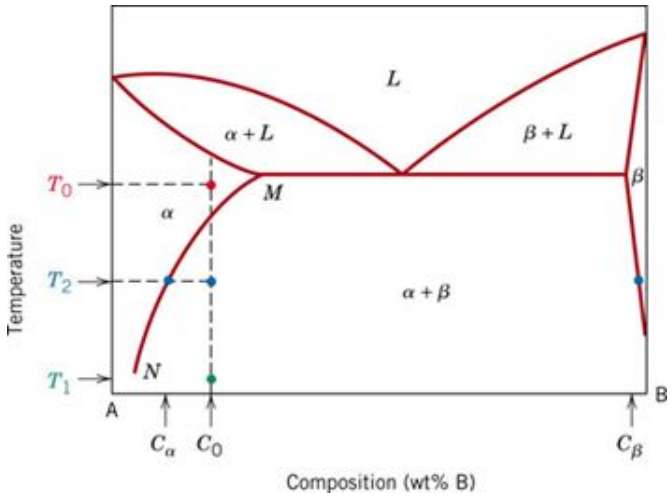

Fig. 4: Al-Cu phase diagram

Once the material has been brought to T2, the beta particles are dispersed in the solid solution - they remain in the same place after quenching. After bringing it up to T1, the beta particles slowly diffuse through the material. The beta particles in our alloy were magnesium which is smaller than aluminum. This results in a tensile stress around each particle. The magnesium particles are distributed across the material and their local

stresses prevent dislocations from moving past them thereby increasing the material's resistance to plastic deformation and thus strength. In a precipitated sample there are two mechanisms which relate to the secondary particle impeding dislocation motion,cutting and bowing. In order for the dislocation to travel past the particle it must either cut through it or bow around it, both of which require much more stress than normal travel. The optimal distribution of magnesium particles for strength as a function of time can be seen in **(Fig. 5)**

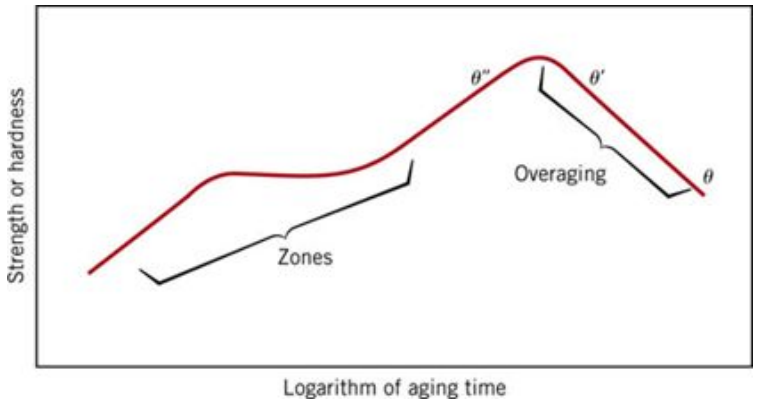

Fig. 5: precipitation hardening behaviour

This plot shows how, after the initial solution heat treatment and quenching, the strength of the material increases as it is "aged" and the beta particles are distributed. At a certain point however the material can be overaged and lose strength. This is because the beta particles that pin dislocations group together and affect fewer and fewer dislocations.

We also performed tensile tests on 1018 annealed steel that was heated to 700^{0}F and 925^{0}F. The function of annealing is to relieve introduced stresses which increases softness and ductility and can produce specific, desired microstructures. This process takes place in three phases: recovery, recrystallization, and grain growth. Recovery takes place at only a fraction of the temperature required for annealing. During this period heat energy is used to rearrange dislocations within the material relieving some some stresses and softening the material. Recrystallization takes place at the temperature T_r which lies between $0.3T_m$ and $0.6T_m$ where T_m is the melting temperature of the material. If materials are held at this temperature for one hour, elongated high dislocation density grains will be replaced by small, strain-free, equiaxed grains. Above the critical temperature of the material grain growth takes place. During this time the small grains formed during recrystallization disappear and are replaced with larger, favorably oriented grains. The 700°C sample was heated over the course of one hour in a box furnace. This sample was held at this temperature for three hours and then left in the furnace as it cooled for five additional hours. . The other sample underwent the same

processing at 925℃. The purpose of this test was to compare it to other lab data in order to investigate the impact of different annealing temperatures. The tensile test data was analyzed by examining the ultimate tensile strength, yield strength, Young's modulus, and the strength hardening exponent.

Additionally the effects of annealing on a previously cold rolled sample were also analyzed. This was done by taking a sample from the most cold rolled group of samples collected earlier in this lab as part of studying the effects of introduced stresses on hardness. This most rolled sample was annealed under the same conditions as the tensile testing sample heated at 925℃. The Vickers hardness was found and the value was converted to ultimate tensile strength and yield strength.

By annealing metals an engineer can tune them for a specific application or prepare them for further refining. Through annealing the material becomes softer and more malleable which will allow for metals to be further shaped without failure.

Knowledge of these techniques and properties are crucial to the field of Materials Science since they are required in order to design solutions to problems. A problem may necessitate a material with a high ductility or a material that is able to sustain a certain force without failing. Using relevant processing we can change the mechanical properties of materials to allow for a wider range of solutions or even find a solution where none existed before.

Procedure

Precipitation:

1. We obtained 10 samples of Aluminum 6061 that had been pre-annealed at 413˚C for 2.5 hours then slow cooled to 250˚C for over 3.5 hours
2. We calibrated our Rockwell tests calibrated to the 30T scale **(Table I)**
3. We performed an initial hardness measurement on the 1st sample
4. Using the handbook as reference **(Fig. 10)** we put the remaining samples in the furnace at 550C for 30 minutes, then quenched them in water.
5. Also using the handbook **(Fig. 10)** the remaining samples were put back into the furnace at ~200-270C
6. After 10 minutes we removed a sample and measured its hardness
7. We repeated step 6 until only 2 samples remained.
8. The following day, the 9th sample was removed and we measured its hardness after recalibration at 30T.

9. Approximately one week later we removed the final sample and measured its hardness after recalibration at 30T.

Cold Rolling:

1. We obtained Samples of 6061 Al and 1018 Steel and measured their thickness and widths
2. Then we performed Vickers Hardness tests upon the samples to determine their initial hardnesses
3. We cold rolled these samples with the cold roller in the machine room
4. After rolling we measured the thickness and widths of the samples and then removed and labeled a portion of each sample
5. We repeated steps 3-4 until the Al sample had been rolled 5 times and the steel sample had been rolled 4 times.
6. We mounted our samples in 2 pucks, one for each type of metal
7. We Performed Vickers hardness tests upon our samples

Annealed Steel:

1. We obtained two dog bone samples of 1018 steel which were were cut prior to the start of the lab. One sample had previously been heated to 700℃ over one hour in a box furnace. This sample was held at this temperature for three hours followed by cooling over five hours in the furnace. The other sample underwent the same processing at 925℃.
2. Following annealing, we removed the oxide that had formed on the sample surfaces with sandpaper.
3. We then recorded Gage length, sample width, and sample height for both samples and inputted this data into the tensile testing computer interface.
4. We then then clamped the samples into a universal testing machine from both ends making sure to keep the force on the samples minimal. An extensometer was added and the machine was zeroed.
5. We then performed tensile testing on both samples at a crosshead speed of 0.001 in/sec until fracture occurred. Data collected from the tensile tests was exported and saved as Excel files.
6. A sample of the highest percentage cold worked 1018 steel sample from the cold rolling portion of the experiment was annealed using the same heating procedure at 925℃.
7. After annealing we mounted and polished this r sample and performed Vickers hardness testing on it.

Results and Discussion

Precipitation:

The main decisions the group made for the timing of removing samples and the temperature at which to treat them were from the handbook in the undergrad lab **(Fig. 6)**. The goal was to generate a similar curve of hardness over time so we had to make our time steps the right length to observe the entire curve while not missing the characteristic behaviour.

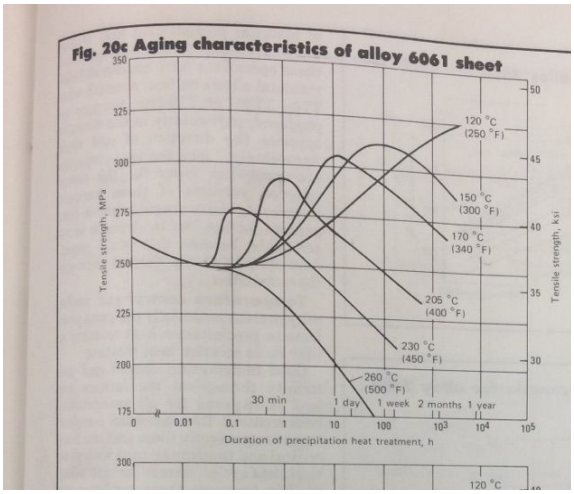

Fig. 6: precipitation hardening isotherms

After the solution hardening and quenching our group started the aging process. **(Fig. 6)** has log(minutes) on the x-axis making it difficult to identify exact numbers so we simply used our best estimates. After deciding on ~220C we found that the temperature in the furnace fluctuated wildly, potentially introducing error.

Our group did not take measurements of a sample at 0 minutes or any data points of a room-temperature sample alongside the heat-treated samples but one can infer from **(Fig.6)** that aging at room temperature for that time would not significantly affect the distribution of the magnesium particles due to the low temperature. The data we collected is seen in **(Table II)** in the appendix as well as **(Fig. 7)**

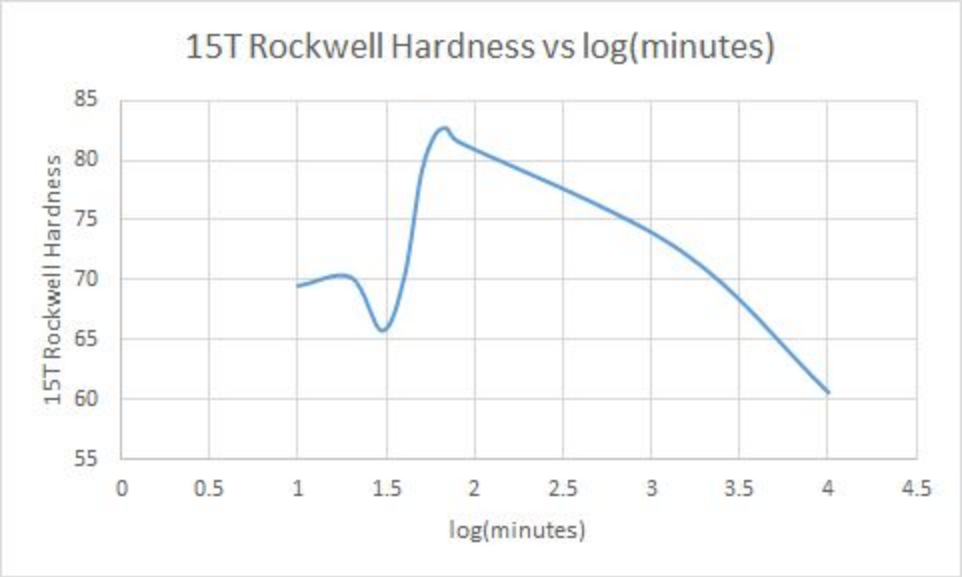

Fig. 7: collected precipitation hardening data

Our group had values of hardness on the Rockwell scale, calibrated at 30T (measurements in appendix), taken at 15T for each of our samples. One can see from **(Fig. 7)** that we observe a similar pattern in our hardness values over time matching what we expected from **(Fig.6)**. Sources of error were the significant fluctuations in temperature during the ageing process.

Our obtained values of hardness are similar to the values from lab group 2D's Lab 2, of 79.7 15T HRB. As expected our hardness after solution hardening was lower. The peak of the curve, what we expect to match this value of as-received steel, is close to our value. Our largest data point is around the peak hardness value; 82.6 is 3.6% greater than the previous as-received hardness value. Part of this could be accounted for if the previous sample had been aged, slightly lowering its hardness. The literature value for the hardness of as-received 6061 Aluminum is 82 HRB which is only 0.8% fewer a difference that can be attributed to a slight calibration error.

Cold Rolling:

From the dimensional data we recorded after each step of cold working our samples **(Tables III & IV)** we used **(Eq. 2)** to calculate the percent our sample had been cold worked.

$$\%CW = \frac{A_0 - A_d}{A_0} x100 \quad \textbf{[2]}$$

Where A_0 &, A_d = cross sectional areas, %CW = Percent cold worked

After vickers analysis was conducted on our samples; we found average values and their corresponding standard deviations for the Vickers Hardness (HV) of our samples **(Tables IV & VI)**. The impact of cold working both the 1018 Steel and 6061 Aluminum samples can be observed in **(Fig.8 & Fig.9)** wherein we plotted the average HV values against the percent cold worked for each sample. We only obtained HV calculations for the first and final two workings for each sample.

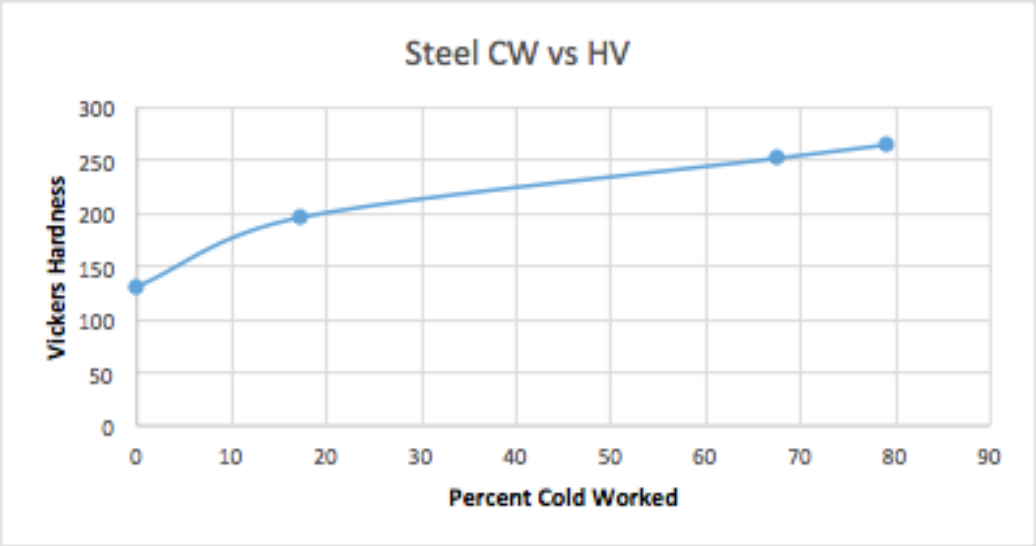

FIg. 8: Percent Cold Worked vs. Vickers Hardness for 1018 Steel

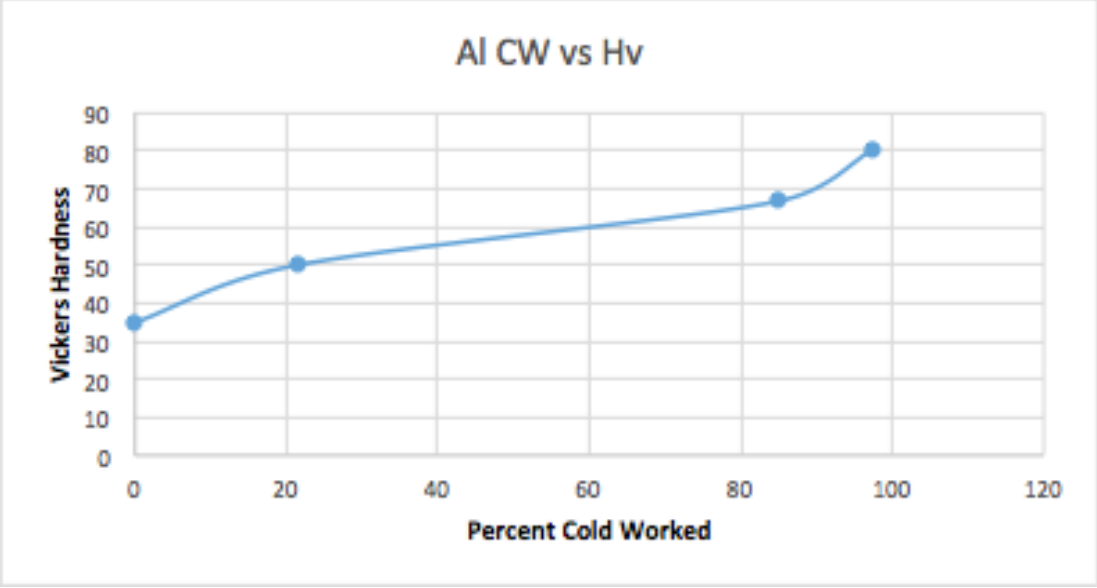

Fig. 9: Percent Cold Worked vs. Vickers Hardness for Aluminum 6061

(Fig.8 & Fig.9) show the clear impact that cold working has on a material. As expected the more cold worked a sample is the greater its hardness becomes and there was no significant difference between the impact of cold rolling on Aluminum 6061 and 1018 Steel.

This rise in hardness is the result of the dislocation frequency increase that cold rolling causes. As the metal is plastically deformed, and its overall area increases, its microstructure changes in several ways. Through the visual differences from **(Img. 1) → (img. 4)** one can clearly observe that not only does cold rolling a sample increase the density of grains and reduce their size, it also dramatically changes their shape as they become increasingly elongated with each roll.[1] The orientation of the grain elongation is in line with the direction the samples were placed into the cold rolling machine.

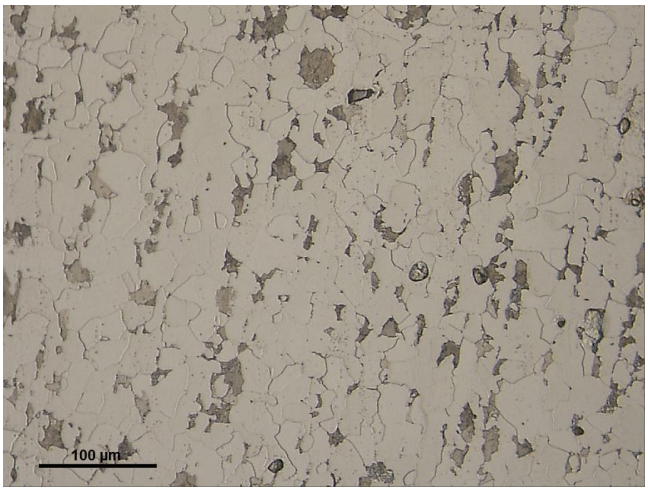	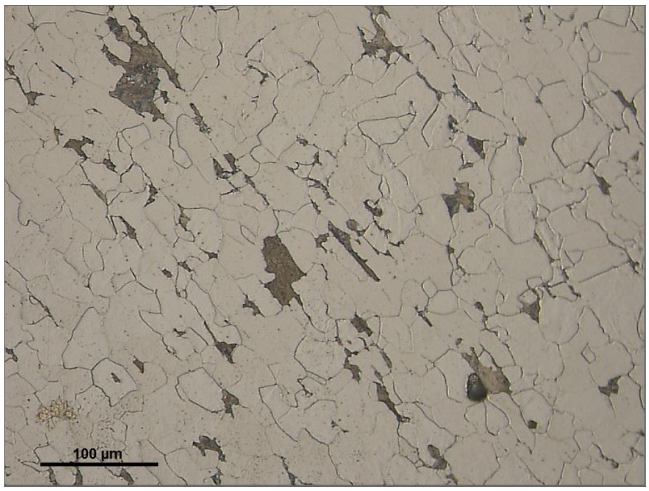
Img.1 - 1018 Steel CW 1x	**Img.2 - 1018 Steel CW 2x**

[1] Our lab group mounted our samples transversely and therefore couldn't observe the impact of CW on the grains of our sample. Because of this we used the steel 1018 images from Maria's Lab group. We therefore do not have any grain number data. Additionally we were unable to find any images of aluminum 6061 with clearly defined grains.

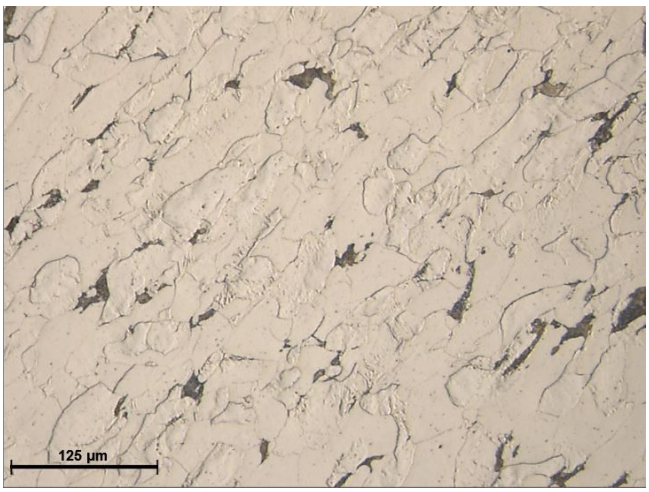	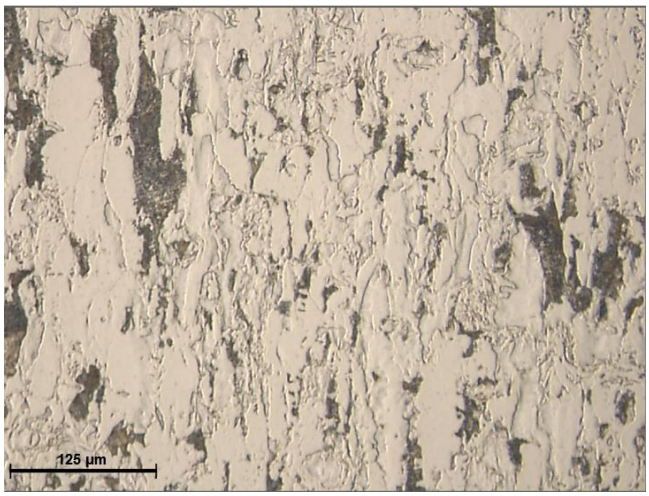
Img.3 - 1018 Steel CW 3x	**Img.4 - 1018 Steel CW 4x**

These changes in the shape and number of grains directly induces the hall petch hardening discussed earlier and the extent that the material has been strain hardened can be calculated with (Eq. 1) but for reasons explained in the footnote above, we were unable to do so. This hardening as a result of an increase in grain density can be in part reversed through annealing, the experimental efficacy of which on our sample is discussed in detail further in the paper.

Annealed Steel:

Tensile testing data was analyzed using a stress-strain curves and the equations utilized in Lab 2. Using the methods learned in Lab 2, we determined the UTS, yield strength, Young's modulus, and strain hardening exponent. By analyzing these four factors we will be able to compare the effects that annealing has on a metal at two different temperature.

(Fig.1) shows the stress-strain curve created using the data the 700℃ sample. The ultimate tensile strength(UTS) was determined by locating the maximum stress attained during the course of testing. For the 700℃ sample this was determined to be 454 MPa. The literature values for annealed 1018 steel are not available so the values for annealed 1020 steel were found due to the very close carbon content.[1] The literature value of the UTS of annealed 1020 steel was 395 MPa yielding a 14.9% error in our experimental value. The Young's modulus was found using the equation. **(Eq. 3)**on all points in the linear elastic region and then taking the average of these values.

$$E = \frac{\delta}{\varepsilon} \quad \textbf{[3]}$$

Where E = elastic modulus , δ = engineering stress, and ε = engineering strain

The Young's modulus for this samples was determined to be 206.85 GPa with a standard deviation of 2.60 GPa using this method. The literature value was 186 GPa giving us an error of 11.2%. The yield strength(YS) was found by finding the point of interception between the stress-strain curve and a line with slope equal to the Young's modulus and a x-intercept of 0.002. Using this we determined the YS to be 362 MPa. The YS given in the literature for annealed 2020 steel was 295 MPa giving an error of 22.7%.

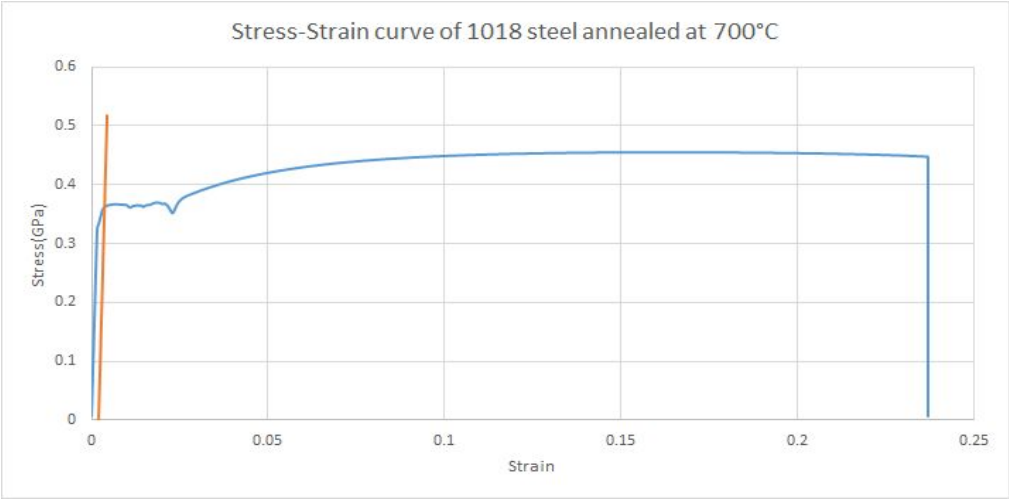

Fig. 10: Stress-strain curve of the sample annealed at 700℃. The orange line represents the 0.2% yield point.

The true stress of the 700℃ was calculated using (Eq.4) and the true strain of the sample was calculated using **(Eq. 5)**

$$\delta_t = \sigma(1+\varepsilon) \quad \textbf{[4]}$$

Where δ t is the true stress, σ is the engineering stress, and ε is engineering strain

$$\varepsilon_t = ln(1+\varepsilon) \quad \textbf{[5]}$$

Where ε_t is the true strain and ε is engineering strain

The true stress- true strain curve is shown in **(Fig. 11)**.

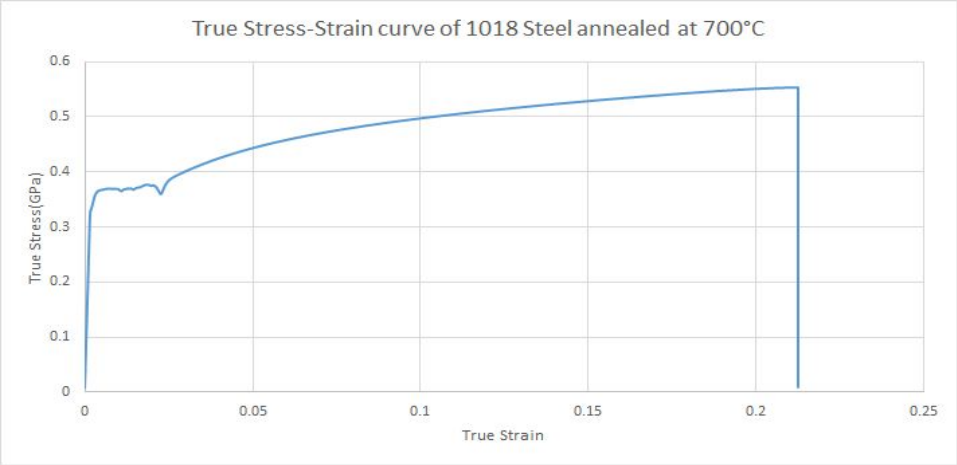

Fig. 11: The true stress-true strain curve of the steel sample heated at 700℃.

The strain hardening exponent was determined using **(Eq. 6).**

$$\ln(\delta_t) = \ln(K) + n * \ln(\varepsilon_t) \quad \textbf{[6]}$$

Where ε_t is the true strain, δ_t is engineering strain, K is the strength index, and n is the strain hardening exponent

A log graph, **(Fig. 12)**, was created using the natural logs of the true stress and true strain. A linear equation was fitted to the portion of the graph corresponding to the end of the yield point extension and the beginning of necking. The slope of this line is equal to the strain hardening exponent and here equaled 0.1731. The literature value for the strain hardening exponent for annealed 1018 steel was found to be 0.25 giving an error of 30.8%.[2]

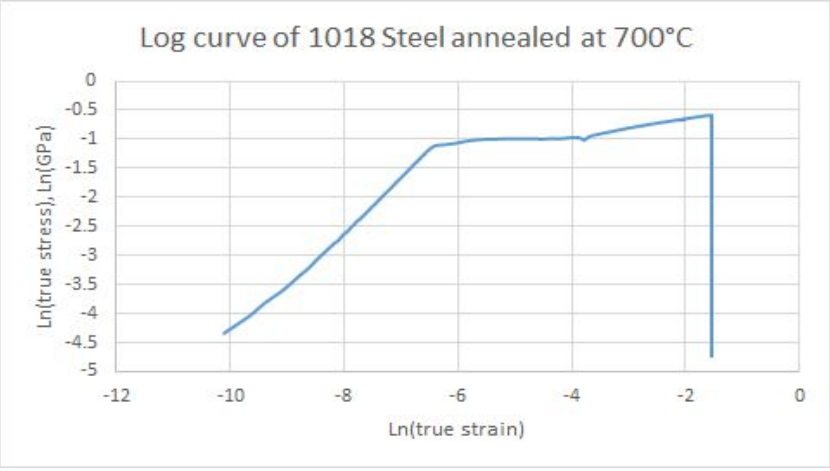

Fig. 12: Logarithmic curve of the true stress and true strain for 1018 steel sample heated at 700℃.

The YS and UTS of the 700℃ was actually much closer to the YS and UTS of cold drawn 1018 steel than to annealed 1020 steel. The literature YS and UTS of 1018 cold drawn steel is 370 MPa and 440 MPa which would give us experimental errors of only 2.2% and 3.2%.[3]

The same procedure was performed on the sample heated at 925℃. The stress-strain curve found for the 925℃ annealed sample is shown in **(Fig. 13)** The UTS was determined to be 388.54 MPa yielding an error of 1.65% compared to the literature value of annealed 1020 steel. The average Young's modulus of was 204.32 GPa with a standard deviation of 2.96 GPa which gives an error of 9.8%. YS was again found using the 0.2% strain method and was determined to be 260.7 MPa which gives an 11.6% error.

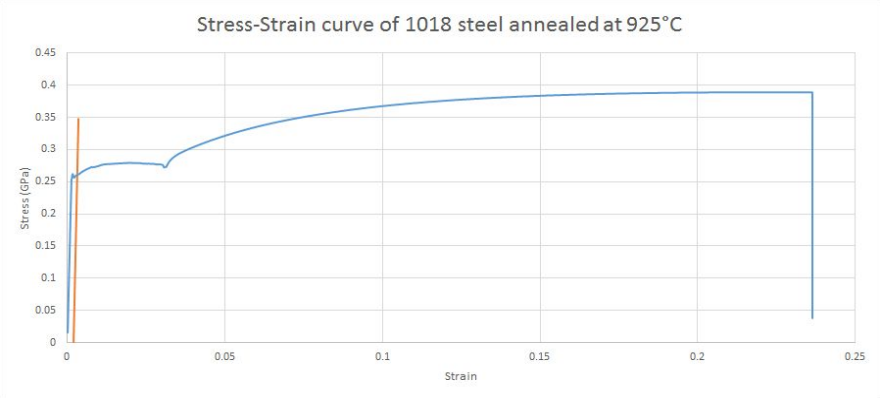

Fig. 13: Stress-strain curve of the sample annealed at 925℃. The orange line represents the 0.2% yield point.

The true stress and true strain were again found using **(Eq. 4)** and **(Eq. 5)**which produced the the stress-strain curve seen in **(Fig. 14)**.

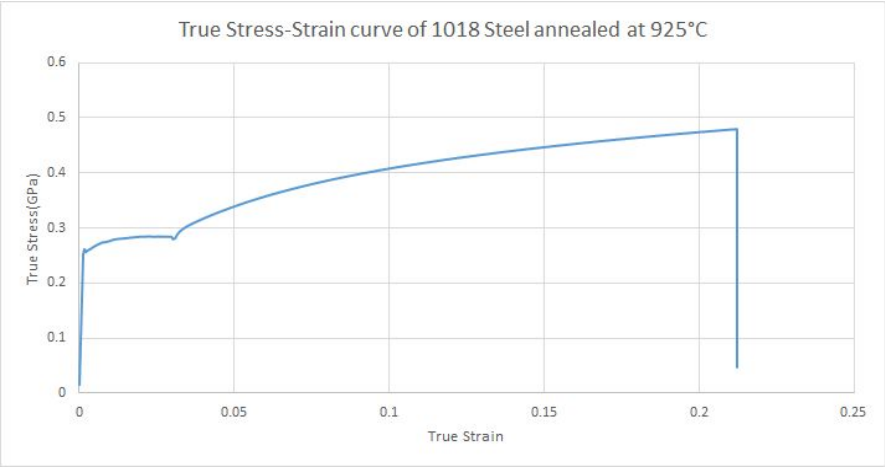

Fig. 14: The true stress-true strain curve of the steel sample heated at 925℃.

The corresponding logarithmic curve is presented in (Fig. 15). The work hardening exponent was found to be 0.2525. The experimental value yielded an error of only 1% compared to the literature value of 0.25 for annealed 1018 steel.

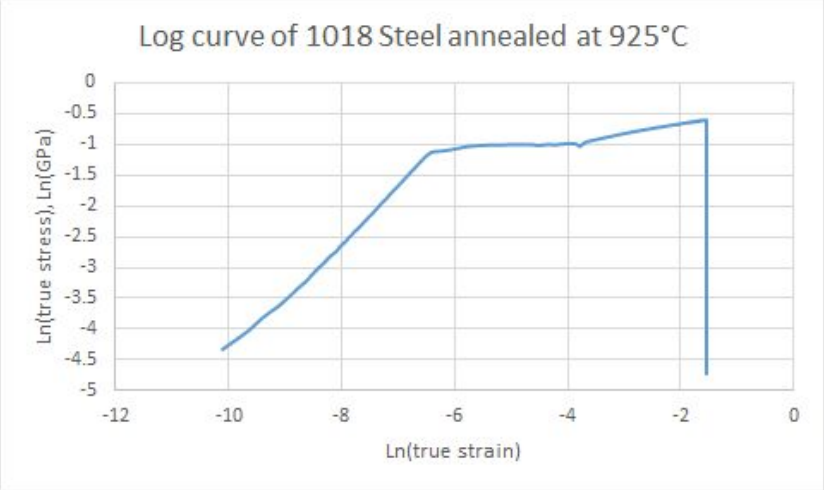

Fig 15: Logarithmic curve of the true stress and true strain for 1018 steel sample heated at 925℃.

The % elongation of both samples was 26% which does not seem to fit with the general trend of the other mechanical properties. The trend should have continued with the sample heated at the higher temperature having an increased % elongation as it was a softer material than the sample heated at 700℃. These values lay in between the percent elongations seen in cold drawn 1018 steel, 15%, and annealed 1020 steel, 36.5%.

The Vickers hardness of our most cold rolled steel sample after annealing at 925℃ was also measured. The average Vickers hardness of five tests was 119.4 with a standard deviation of 4.03. This value was converted to a Brinell hardness of 119 as per ASTM standard E140.[2] The vickers hardness value given for annealed 1020 steel was 111 which yields an error of 7.2%. The Brinell hardness value was then used to find the UTS and YS using **(Eq. 6)** and **(Eq. 7)** respectively. The UTS determined to be 402.22 MPa and the YS to be 252.7 MPa.

$$TS(MPa) = 3.55 * HB \quad \textbf{[6]}$$

Where TS = ultimate tensile strength and HB = Brinell hardness

$$YS = -90.7 + (2.876 * HV) \quad \textbf{[7]}$$

Wherein YS = Yield Strength and HV = Vickers Hardness

The purpose of annealing is to relieve stresses, increase ductility, and to achieve a specified microstructure. Full annealing requires gradual heating above a material's recrystallization temperature for a period of time. If the the temperature is not above the recrystallization temperature then the process stops before grain growth occurs, leaving a large number of small, stress free grains. The recrystallization temperature of 1018 steel is determined by the temperature at which austenite forms for the given carbon concentration. At 0.18% carbon the temperature at which austenite forms is 727℃. This is why the sample annealed at 700℃ has such a large error compared to the other sample. Because it was heated below the recrystallization temperature, the 700℃ sample was not fully annealed and retained its smaller grain structure. This smaller grain structure is directly responsible for the 16.86% higher UTS and 75.13% higher YS in the 700℃ sample than in the 925℃ sample.

The cold worked sample that was heated under the same conditions as the 925℃ sample showed very similar UTS and YS values. This means that the grain structure of the highly cold worked sample was returned to its pre-rolled condition. In addition, dislocation density would be reverted to normal as the introduced stress are annihilated by crystal recombination. The act of full annealing effectively reversed all effects done by cold rolling aside from the change in cross sectional area. This is evident in the fact that the annealed after cold rolling sample and the plain annealed sample have UTSs and YSs within only around 14 MPa.

Several potential sources of error exist which could have affected our results. We saw from the precipitation experiment that the temperature in the box furnaces had a tendency to fluctuate roughly thirty degrees from the set temperature. Because of this, the temperatures that samples were annealed at could have been higher or lower than the reported temperature. This could have yielded samples that were not fully annealed. Another source of error could be an issue with the reported gage length. The gage length of the tensile was always assumed to be one inch but was never measured. If this assumption proved to be false then our calculations would contain a large degree of error.

Appendix

Tables:

Table I: 30T Rockwell calibration

30T:
47.6
48.2
47.3

(Accepted value: 46.1 +/- 1.5)

Table II: Precipitation Hardening Data

Log(min)	1	1.30103	1.477121	1.60206	1.69897	1.778151	1.845098	1.90309	3.158362	4.003461
min	10	20	30	40	50	60	70	80	1440	10080
H1	68.8	70.5	65.1	69.5	78	82.4	82.2	81.5	73.2	60.6
H2	70.1	70.8	66.5	71.2	79.6	82.7	83.1	81.9	72.4	60.8
H3	69.6	69.3	65.6	70	79.3	81.5	82.7	81.4	72	60.3
Avg H	69.5	70.2	65.73333	70.23333	78.96667	82.2	82.66667	81.6	72.53333	60.56667

Table III*: Steel 1018 Cold Rolling*

Roll	Width(mm)	Thickness(mm)		Area(mm^2)		%CW
0	31.69	7.9		250.351		0
1	32.17	6.45		207.4965		17.11776666
2	33.58	4.75		159.505		36.28745242
3	36.1	2.25		81.225		67.555552
4	1.4	37.5		52.5		79.02944266

Table IV*: Aluminum 6061 Cold Rolling*

Roll	Width(mm)	Thickness(mm)		Area(mm^2)		%CW
0	25.33	7.93		200.8669		0
1	25.7	6.14		157.798		21.44151177
2	26.11	4.8		125.328		37.60644486
3	26.2	2.25		58.95		70.652208
4	27.6	1.1		30.36		84.88551374
5	28	0.2		5.6		97.21208

Table V: *Steel 1018 Hardness*

Roll	Avg. HV	Stdev
0	129.75	1.299038106
1	196	2.34520788
2	n/a	n/a
3	252	5.522680509
4	264.5	1.5

Table VI: *Aluminum 6061 Hardness*

Roll	Avg. HV	Stdev
0	34.8	1.469693846
1	50	2.236067977
2	n/a	n/a
3	n/a	n/a
4	66.75	2.680951324
5	80.2	4.53431362

Works Cited

1. http://www.matweb.com/search/DataSheet.aspx?MatGUID=3e8a4ed96e5f4f16923ec21e95b69585&ckck=1
2. Datsko, Joseph. *Materials Properties and Manufacturing Process.* New York: John Wiley & Sons, Inc. , p 21.
3. http://www.matweb.com/search/datasheet_print.aspx?matguid=3a9cc570fbb24d119f08db22a53e2421
4. ‘‘Hardness Conversion Tables for Metals Relationship Among Brinell Hardness, Vickers Hardness, Rockwell Hardness, Superficial Hardness, Knoop Hardness, and Scleroscope Hardness,’’ E 140-05 2005, Annual Book of ASTM Standards, vol. 3.01. American Society for Testing and Materials, West Conshokocken, Pennsylvania, USA, p 139-140.
5. http://www.substech.com/dokuwiki/doku.php?id=iron-carbon_phase_diagram